

# Causes of Missing Dots in Rotogravure Printing

*Martorana, E., Ziegler, H., a Campo, F.W. and Jühe, H.-H.: University of Applied Sciences - München and Stora Enso Research Center Mönchengladbach*

Published in: Wochenblatt für Papierfabrikation 134, No. 11-12, pp. 690-698 (2006)

## Abstract

This work has shown that the number of local defects (craters) beyond certain limit values correlates very well with the number of missing dots, and therefore the surface topography of the paper has definitely the greatest impact on printability in rotogravure. The deepenings have an average depth of 2-5  $\mu\text{m}$  and diameters between 50-250  $\mu\text{m}$ . When ESA is used bigger craters as regards depth and diameter are necessary to cause missing dots. However, not all missing dots can be explained and described by means of surface topography. Non-topographic factors, such as electric properties of papers (especially when using the ESA), fibre and filler distribution, ink absorbency or microscopic compressibility can also have an influence on printability as regards missing dots. Paper independent factors (e.g. printing ink or printing machine) may also have a certain influence on missing dots.

Keywords: missing dots, printability, rotogravure, topography, craters, sc-paper, smoothness, roughness, ESA

## 1 Introduction

Due to increasing cost pressure, paper producers and print shops are continually forced to produce at a lower cost. The increased speed of print and paper machines, as well as the steadily increasing demands as regards print quality and optical paper properties, thrust the topic of missing dots more and more into the foreground. Without doubt, smoothness of the paper is a key parameter in rotogravure printing, in order to achieve a good ink transfer to the paper. But is not sufficient to determine only the smoothness of a paper when estimating its printability in the rotogravure process. In fact, printability is a complex quality parameter which depends on many paper properties, and which is still very difficult for the paper-makers to measure. Many attempts to correlate missing dots to individual paper properties failed because, in general, there is no significant correlation between missing dots and other physical properties of the paper, such as smoothness, compressibility, porosity, ink absorbency, or even electrostatic properties.

It is now known that local structures in the paper surface, such as crater-shaped pits or borders of fibres, cause a missing dot in exactly the place where they occur. However, for some time, it has been possible to measure these local defects in the paper surface by means of optical profiling devices (confocal scanning laser microscopes). The traditional measuring devices, such as air-leak methods, have too large measuring areas to determine the local defects (craters) which cause missing dots.

Objective of this work at the Stora Enso Research Center Mönchengladbach was to find significant correlations between missing dots and surface structures of the paper. Furthermore the local defects causing missing dots (craters) should be characterised and described as regards their form and size. For the deepenings in the paper surface connected with missing dots the name “crater” has become familiar [1], and it is used in this report, too. However, it should be stated very clearly that these deepenings must not necessarily be surface structures surrounded by a closed wall. Other structures can also be found, e.g. steps or bays.

## 2 Electrostatic assistance and causes of missing dots

### 2.1 Electrostatic assist (ESA)

With the application of the electrostatic assist, the number of missing dots can be reduced significantly.

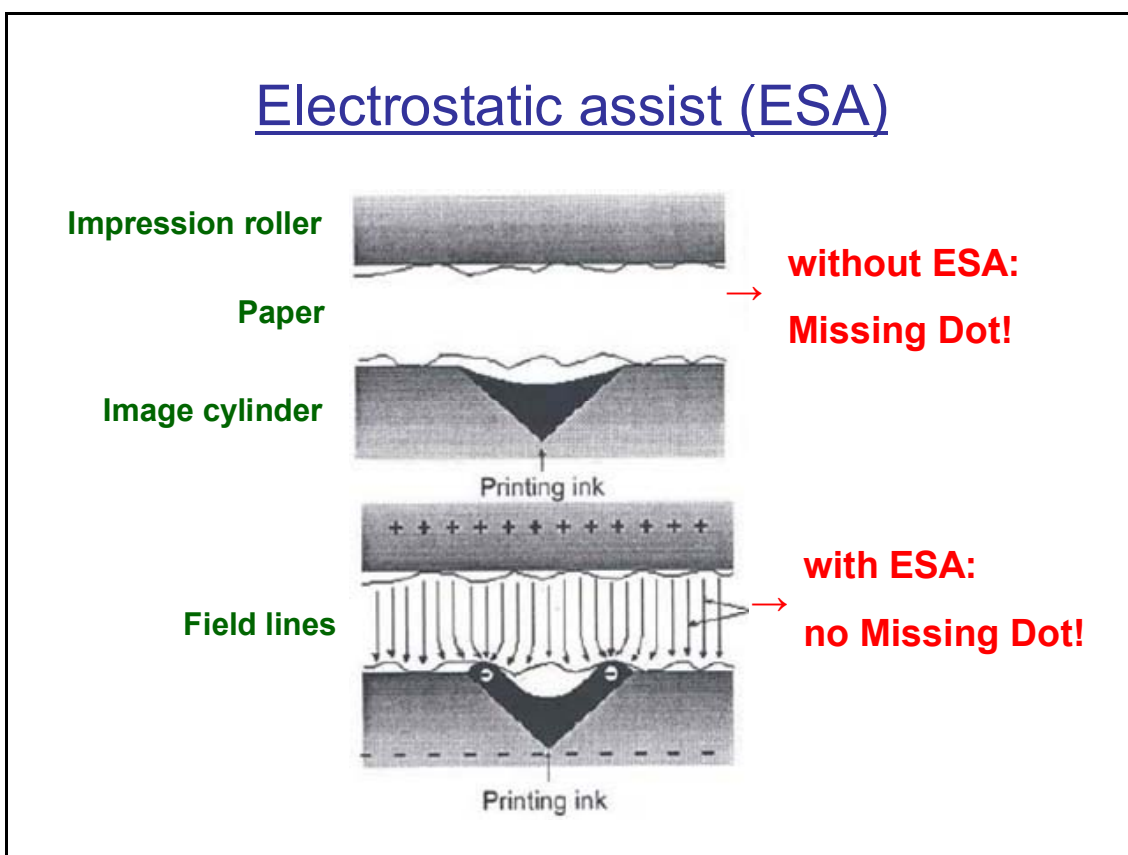


**Figure 1: Ink transfer und mechanism of the electrostatic assistance**

Figure 1 shows the difference when printing with and without electrostatic assist, as well as the behaviour of the printing ink during electrostatic charging. The meniscus of the ink in the pit is caused by the surface tension. When the electric field is generated the printing ink rises at the walls of the pit. By the application of the electric field it is possible to support the ink transfer onto the paper surface tremendously.

## 2.2 Causes of missing dots

According to Praast and Göttsching bekk smoothness correlates only to a certain extent with the number of missing dots. Especially if papers have a bekk smoothness of 800 s or higher, there is no longer a connection to the number of missing dots. However, there is a significant influence of mass variations in the paper on the number of missing dots. Thus, missing dots basically occur at areas of lower grammage [12].

Correlations of missing dots to PPS-Roughness and Heliotest are not very strong and disappear when electrostatic assist (ESA) is used. Thus, it is assumed that also the electric properties of the paper have an influence on the ink transfer in rotogravure when using the ESA [5]. Therefore it is assumed that a highly-conductive paper impairs the electric field of the ESA and reduces the probability of missing dots.

According to Neß the surface structure of the paper has the greatest impact on missing dots in rotogravure printing. The local roughness calculated from the surface profile of the paper, correlates very strong to the missing area of the printing dots and gives far better differentiation than Bekk or PPS, especially in a narrow quality spectrum [10].

According to Antoine 98 % of all missing dots can be explained by deepening (crater-shaped pits) in the paper surface. The main causes for these deepening are large fibres, fibre borders, fibre crossings and pigment agglomerates. On 78 % of the craters at least one fibre is bordering, on 50 % at least two or even more fibres. In 43 % of the cases pigment agglomerates are present. Of course, large fibres and fibre crossings can be seen in well printed areas, too. However, there the local deepening are filled out by pigments. The application of the electrostatic assist is another important factor as regards the causes of missing dots. When ESA is used, the printing ink can be transferred into deeper craters of the paper [2].

According to Jühe the macroscopic compressibility of SC-paper has no impact on the number of missing dots, due to the fact that the impression cylinder is much stronger compressible in z-direction than the paper [7].

Figure 2 shall summarise and make clear how complex the topic of missing dots is, and that only one factor (topography) of many other possible influencing factors was investigated in this work.

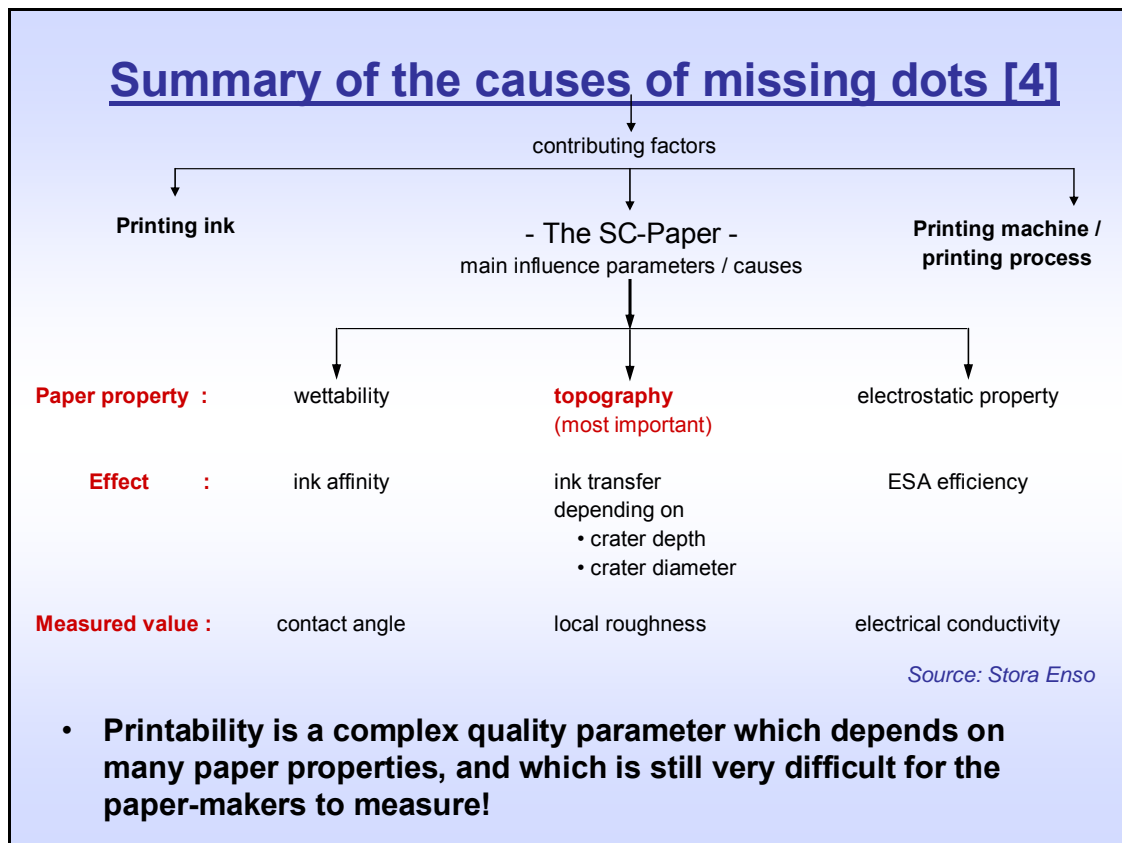


Figure 2: Causes of missing dots [4]

### 3 Can rotogravure printability be measured already on the paper?

#### 3.1 Classical measuring methods

Air-leak measuring devices have been used for a long time in the paper industry to determine smoothness. The smoothness is described as a function of the air flow along the paper surface. The most common instruments are Bekk, Bendtsen and Parker Print-Surf. The problem is that all these instruments allow only an indirect measurement of the smoothness [14]. Bekk and Bendtsen are able to estimate the increase of smoothness after calendering. However, the correlation to the printability is not very strong. This can be explained due to the fact that the thickness of the rings of the Bekk and Bendtsen measuring systems are respectively 13.05 mm and 0.15 mm, while the minimum printing dots have diameters of approximately 0.01–0.02 mm. The PPS equipment measures the surface with a 0.051 mm wide ring, which is much closer to the range of dots used by rotogravure [13]. However, the PPS measurement is still insufficient to determine differences of the paper surface in the range of printing dots, and therefore to draw clear conclusions as regards printability. Only papers of similar quality can be compared.

#### 3.2 Optical measuring methods

Smoothness measurements using air-leak methods reduce the analysis of the paper surface to one single value. Due to the large measuring areas, small, local

deepenings do not appear in the final result. But precisely these local defects are the main cause of missing dots in rotogravure printing. Optical profiling devices such as confocal laser microscopes have focus diameters of 1  $\mu\text{m}$  and resolutions in z-direction of 0.01  $\mu\text{m}$ . For this reason variations in roughness in the range clearly smaller than printing dots can be detected using optical measuring devices. Thereby the roughness is measured directly and contact-free [11,14].

### 3.2.1 Atos PL $\mu$ : The new topography measurement at Stora Enso Research

In figure 3 a real reproduction of the PL $\mu$  can be seen. Important functional units, such as the CCD-camera, the objectives, the plane-table and the joystick are visible. At Stora Enso Mönchengladbach the plane-table is additionally equipped with an electrostatic paper fastener (not in the figure), which ensures an optimal positioning and fixation of the sample. The joystick and the scrollers are used to move the plane-table, as well as for the adjustment of the focus.



**Figure 3: Optical Profiling device PL $\mu$  [3]**

A confocal laser scanning microscope (CLSM) uses a laser, a confocal lens aperture and a detector to create a confocal image. The laser beam is first widened and then projected from the objective of the microscope onto the sample. The reflected or scattered light passes the same objective again, and reaches the confocal lens aperture and finally the photodetector.

In the PL $\mu$  the aperture of the light source is replaced by a pattern of parallel slits and the photodetector by a CCD-camera. Instead of scanning the confocal information

point by point the PL $\mu$  is able to detect the confocal information of thousands of points simultaneously, which results in a very short measuring time [3]. Figure 4 illustrates the functional principle of the PL $\mu$ .

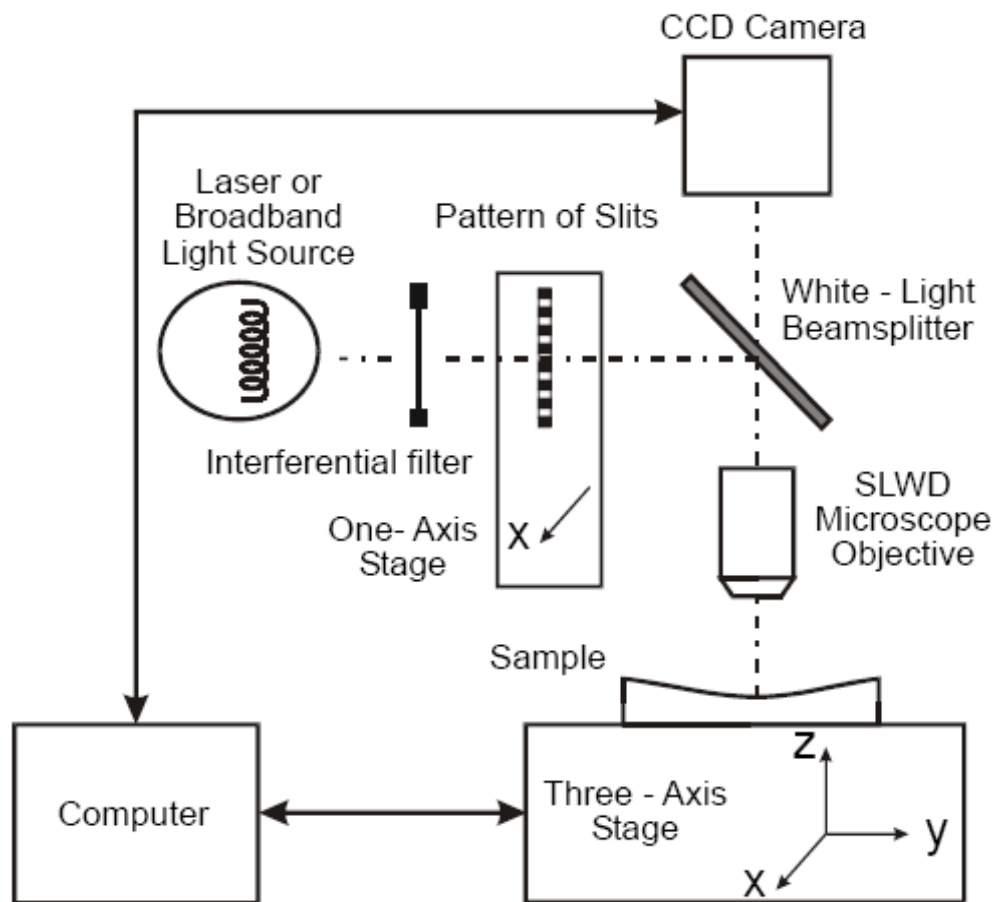
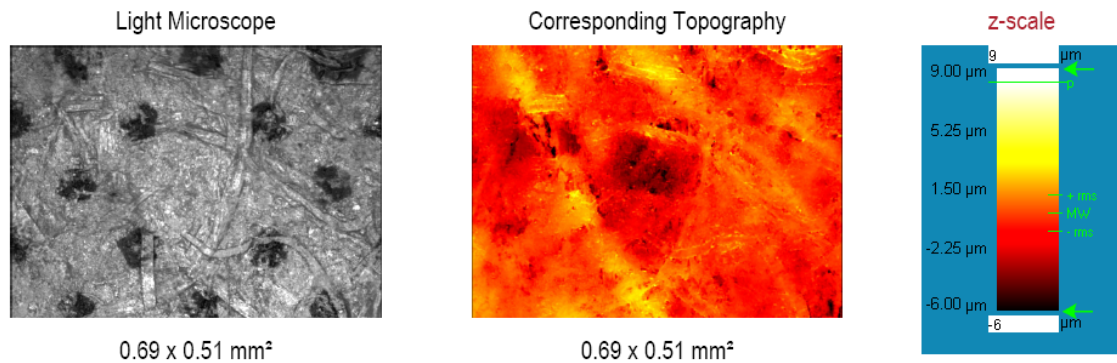


*Figure 4: Functional principle of the PL $\mu$*

### 3.2.2 Measurements with the PL $\mu$

The PL $\mu$  offers a lot of different measuring methods. However, only the measuring methods which are important for this work are briefly described.

The most common measuring procedures are topography and confocal image. The confocal image is a microscopic photo of the sample. The measurement of the topography results in a three-dimensional chart of the sample in the entire lens coverage of the objective.



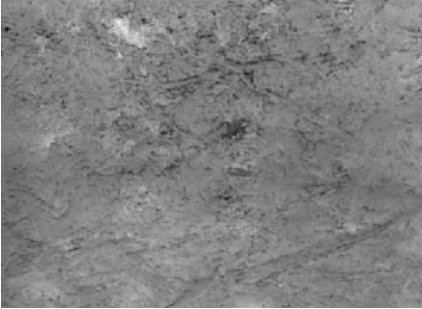
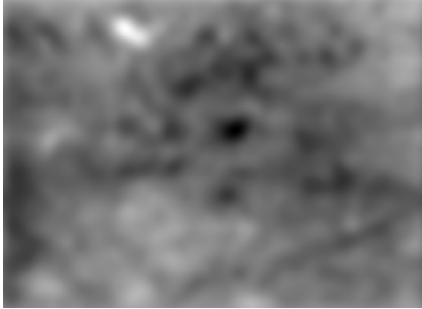
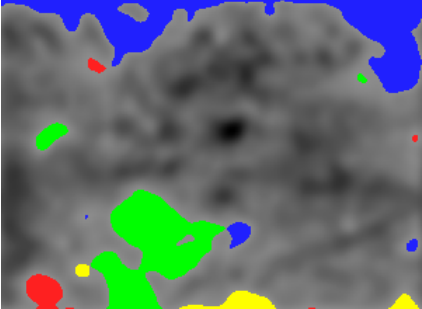
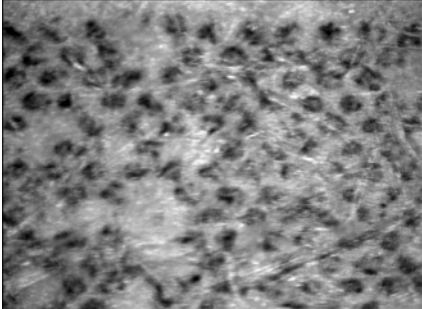
**Figure 5: Confocal image and corresponding topography**

Figure 5 shows a confocal image and the corresponding topography. It can be seen that at the position of the missing dot, a depression in the paper surface occurs, which is additionally surrounded by two or three large fibres.

### 3.2.3 Image editing software ATOS Mark III

The program ATOS Mark III is a software for the analysis of 2D- and 3D-surface data. In the following the main steps of the procedure for the detection of craters in the paper surface, which was developed at Stora Enso Research Mönchengladbach shall be described. Table 1 illustrates the single steps of the crater analysis.

**Table 1: Steps of the crater analysis [1]**

|   |   |
|---|---|
| <p><i>Step 1: Measuring of the topography</i></p>  | <p><i>Step 2: Filtering of the topography</i></p>                   |
| <p><i>Step 3: Detection of the craters</i></p>    | <p><i>Comparison: final print;<br/>Border of the printing</i></p>  |

After the measurement of the topography all topographic variations, which are much smaller than printing dots are filtered out. In the smoothed image the craters are then searched, marked and evaluated as regards their form and size. The values measured at the craters are depth, diameter and volume. The fourth figure shows the final print result. If this figure is compared with the third one it can be seen that in nearly all cases, the software found the craters in the paper surface which have caused missing dots [1].

## 4 Topography analysis

### 4.1 Investigations

At Stora Enso Corporate Research the surface topography of nine SC(A)-papers (sRa 1.0 – 1.3  $\mu\text{m}$ ) from different manufacturers has been investigated by means of the PL $\mu$ -instrument. These papers have been printed on Burda's test rotogravure machine, too.

The printing machine is equipped with an electrostatic assistance of the company Eltex. The machine width is 15 cm and the speed for the trials was 6 m/s. The samples have been printed with three screens (screen 70 stretched, screen 70 upset and screen 100) and four different ESA settings (0 V, 125 V, 180 V and 360 V). The



missing dots of the burda printings were detected with the printability-analyser DA 1 (Dr. Praast) in the 10%-field. The results are shown in table 2.

**Table 2: Number of missing dots per cm<sup>2</sup> in the 10%-field [1]**

| ESA   | Sample:<br>Screen | SC-1 | SC-2 | SC-3 | SC-4 | SC-5 | SC-6 | SC-7 | SC-8 | SC-9 |
|-------|-------------------|------|------|------|------|------|------|------|------|------|
| w/o   | 100               | 1434 | 1660 | 1429 | 1466 | 1801 | 2147 | 2015 | 1906 | 2052 |
|       | 70 up.            | 132  | 254  | 190  | 103  | 256  | 354  | 298  | 331  | 327  |
|       | 70 st.            | 103  | 165  | 113  | 69   | 158  | 230  | 187  | 206  | 209  |
| 125 V | 100               | 1224 | 1430 | 1248 | 1240 | 1366 | 1846 | 1634 | 1422 | 1598 |
|       | 70 up.            | 72   | 142  | 136  | 87   | 109  | 200  | 149  | 151  | 167  |
|       | 70 st.            | 43   | 83   | 69   | 42   | 51   | 122  | 75   | 79   | 92   |
| 180 V | 100               | 688  | 1040 | 1191 | 911  | 943  | 195  | 749  | 576  | 875  |
|       | 70 up.            | 21   | 52   | 81   | 31   | 24   | 0    | 29   | 27   | 35   |
|       | 70 st.            | 11   | 32   | 39   | 11   | 13   | 1    | 21   | 20   | 19   |
| 360 V | 100               | 173  | 155  | 273  | 76   | 140  | 274  | 198  | 213  | 160  |
|       | 70 up.            | 0    | 0,5  | 3    | 0    | 0    | 1    | 0    | 0    | 0    |
|       | 70 st.            | 1    | 1    | 2    | 0    | 0    | 2    | 1    | 1    | 1    |

## 4.2 MD-Topographies

For the measurement of a so called MD-Topography the sample is positioned under the microscope so that the missing dot is located in the center of the measuring field. The aim is to measure exactly that structure which has actually caused a missing dot.

Figure 6 shows the position of the sample when measuring a MD-Topography, as well as three examples.

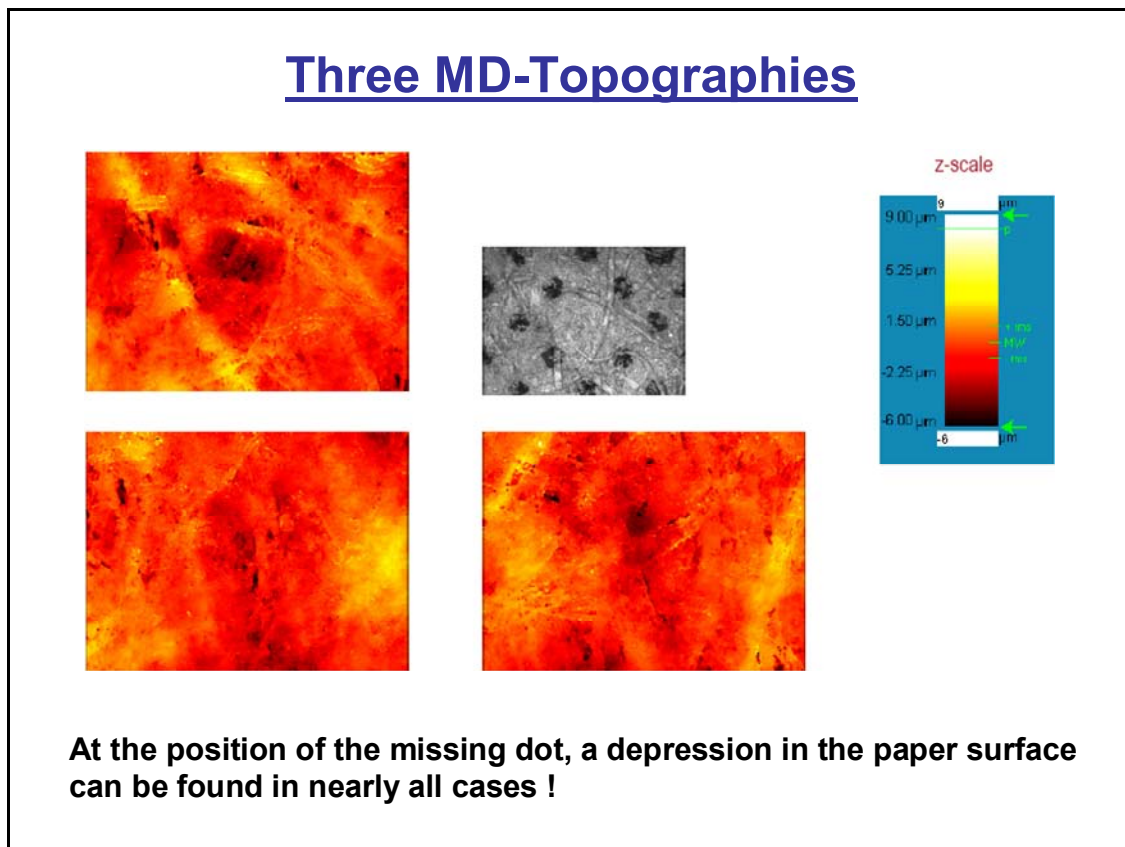


*Figure 6: Position of the missing dot when measuring a MD-Topography*

For every paper, several different MD-Topographies have been measured. The evaluation of the MD-Topographies gives information about the topographic structure which is frequently connected with a missing dot. Especially at higher ESA voltages (360 V) bigger craters, as regards depth and diameter, are necessary to cause missing dots.

#### **4.3 MD-Topography measurements of the burda printings**

Figure 7 shows the maximum depth of the craters in MD-position. The depth of the craters is calculated starting from the topographic zero level.

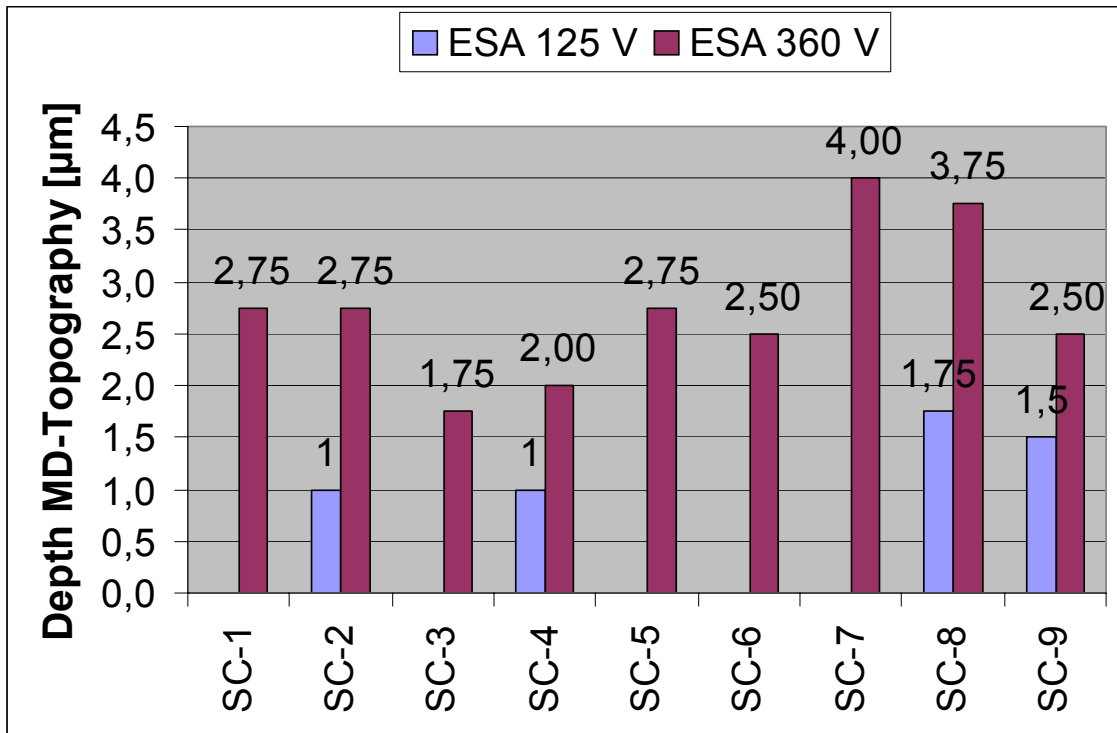


Figure 7: Depth of craters in MD-position of the burda printings [1]

The craters in MD-position are much deeper for ESA 360 V than for ESA 125 V. So to say: the missing dots draw back into deeper craters, if the ESA is running with more power.

Figure 8 shows the connection between the crater depth and the number of missing dots for ESA 360 V (screen 100). It can be seen that the number of missing dots correlates with the crater depth. However, there are two samples which do not follow this rule.

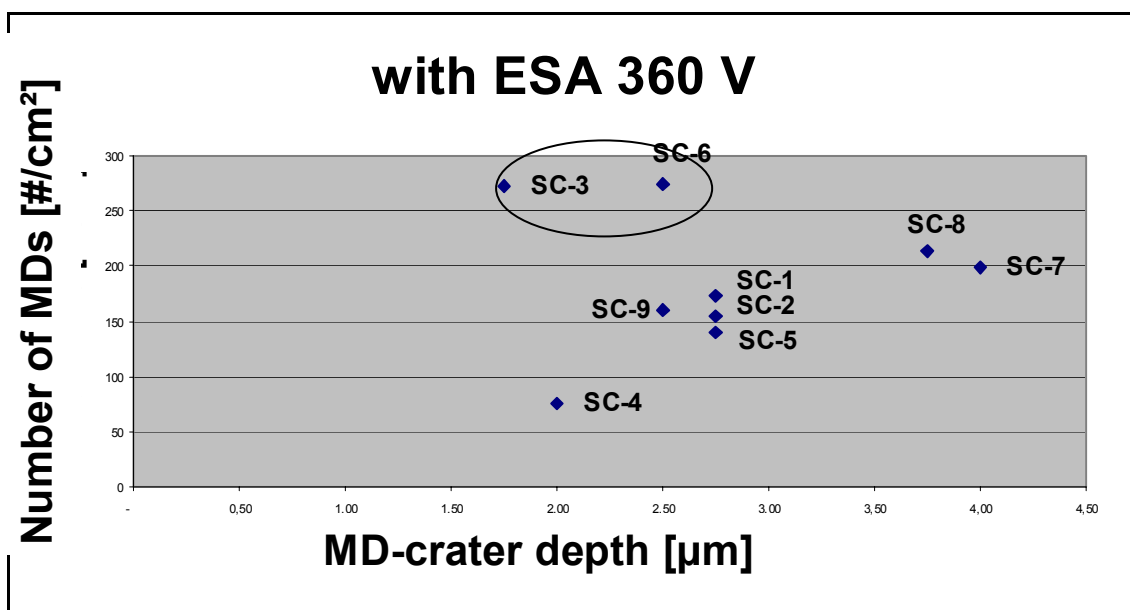
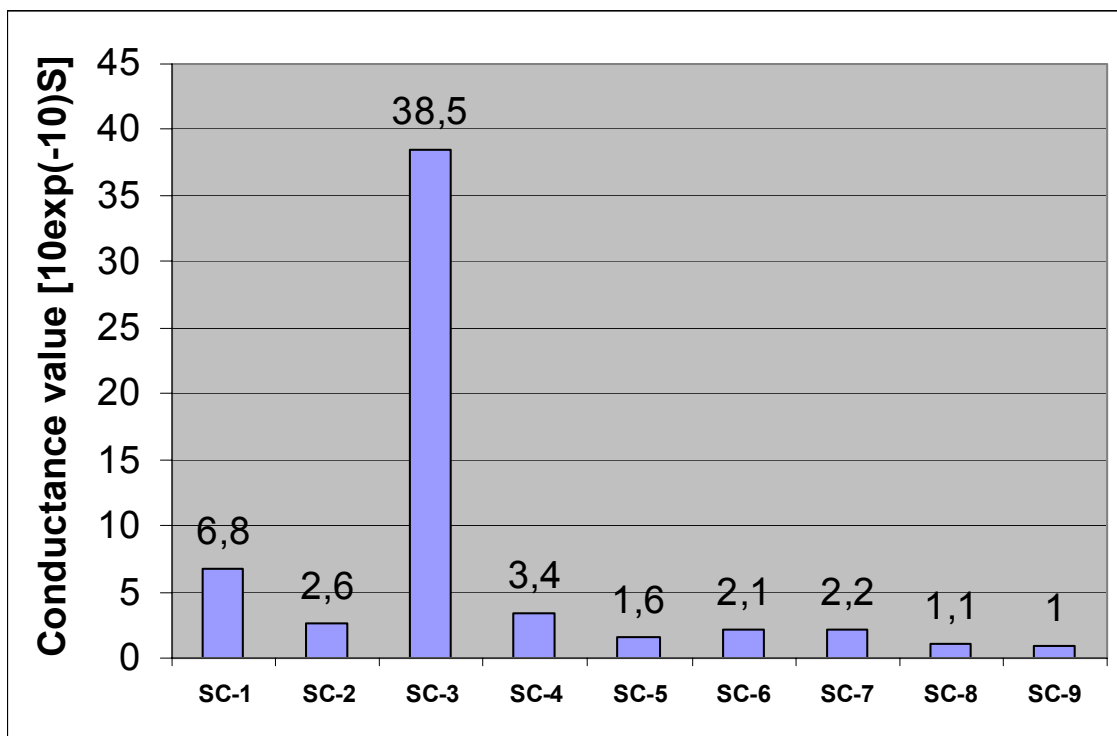


Figure 8: Connection between missing dots and crater depth at ESA 360 V [1]

The two exceptions are the encircled papers SC-3 and SC-6, which differ in some other parameters, too. A possible explanation for this behaviour is that the sample SC-3 shows clearly different electrical properties, which might influence the performance of the ESA. The electrical properties are relevant especially at high ESA-voltages (360V).

Figure 9 shows the electrical conductance value of the samples. It can be seen that the paper SC-3 differs clearly from all other samples.



**Figure 9: Conductance values of the samples**

For the sample SC-6 the number of missing dots at ESA 360 V (screen 100) is higher compared to ESA 180 V (cp. Table 2), which is very unlikely and indicates a failure of the ESA for this paper.

#### 4.4 Crater statistics

The crater statistics are used to correlate the number of missing dots with the number and size (depth, diameter and volume) of craters. Objective of the interpretation of the crater statistics is to forecast the printability of unprinted papers.

Until now only mean values have been considered in the crater statistics. However, not only mean values should be considered in the crater statistics, due to the fact that they contain craters which are too small to influence a printing dot. Therefore the craters were analysed against limit values, too. Figure 10 shows an example for a frequency function. The diameter is shown on the x-axis. On the y-axis the number of craters which have at least the diameter on the x-axis is calculated.

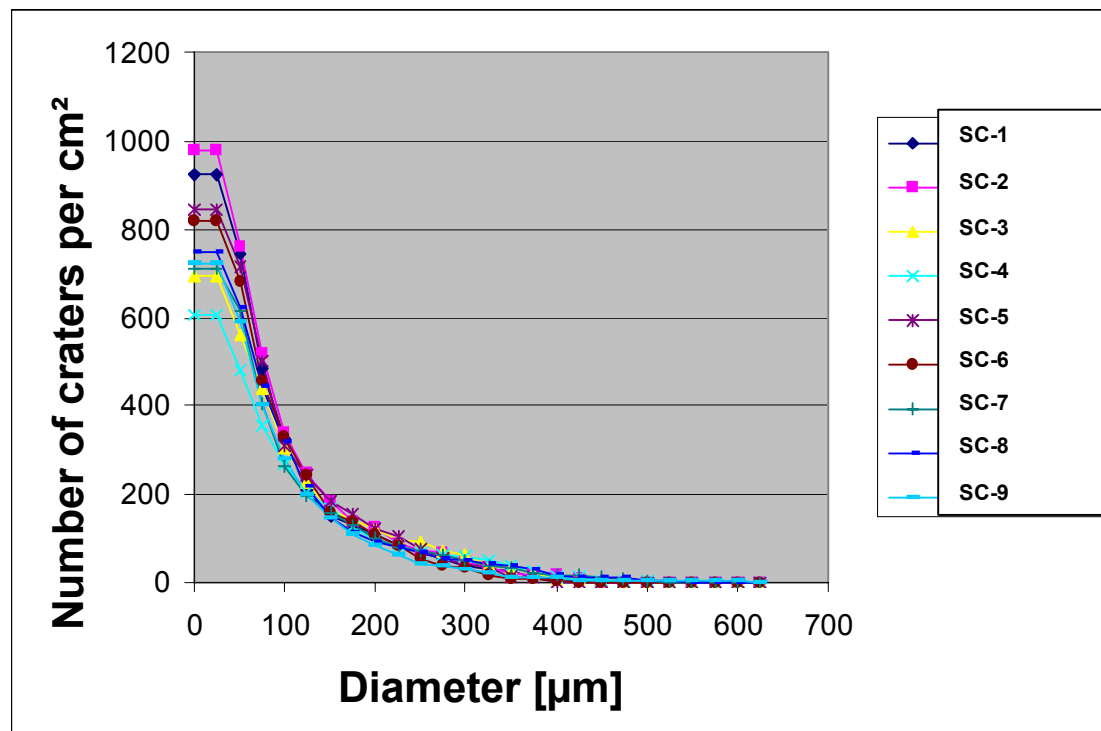


Figure 10: Example for a frequency distribution (topographies  $1.4 \times 1.0 \text{ mm}^2$ ) [1]

The reason for the analysis of frequency functions is that a crater is more likely to cause a missing dot if he is bigger, deeper or wider. If there is a limit value beyond which a crater is more likely to cause a missing dot, this limit value would be identified due to the high correlation with the measured missing dots [1].

The mean values show for some parameters a clear and meaningful connection with the missing dots found in the burda prints. The results regarding frequency functions are not so clear. Some meaningful correlations can be found; however, they are not frequent enough and do not show a reasonable pattern. At this point it was decided to continue the topic within a thesis and realise an advanced analysis of the crater statistics.

## 5 Advanced analysis of the crater statistics

When regarding frequency functions different parameters such as depth, diameter and volume of craters should be combined and correlated to the number of missing dots. Otherwise the frequency functions would be disturbed by many craters with innocuous combinations. It stands to reason that a crater must have a minimum depth and a minimum diameter/-volume to cause a missing dot (→ multiple limit values!)

When two or three limit values are defined in the frequency functions 2D- and 3D-histograms are generated. In these 2D- and 3D-histograms the number of the craters beyond certain limit values are correlated with the number of missing dots. The analysis of the limit values in the multidimensional histograms were done with the high-pass filtered topographies  $8.4 \times 8.4 \text{ mm}^2$ , due to the high numbers of craters found on these topographies.

Figure 11 shall illustrate the investigations in excel by means of multidimensional frequency functions.

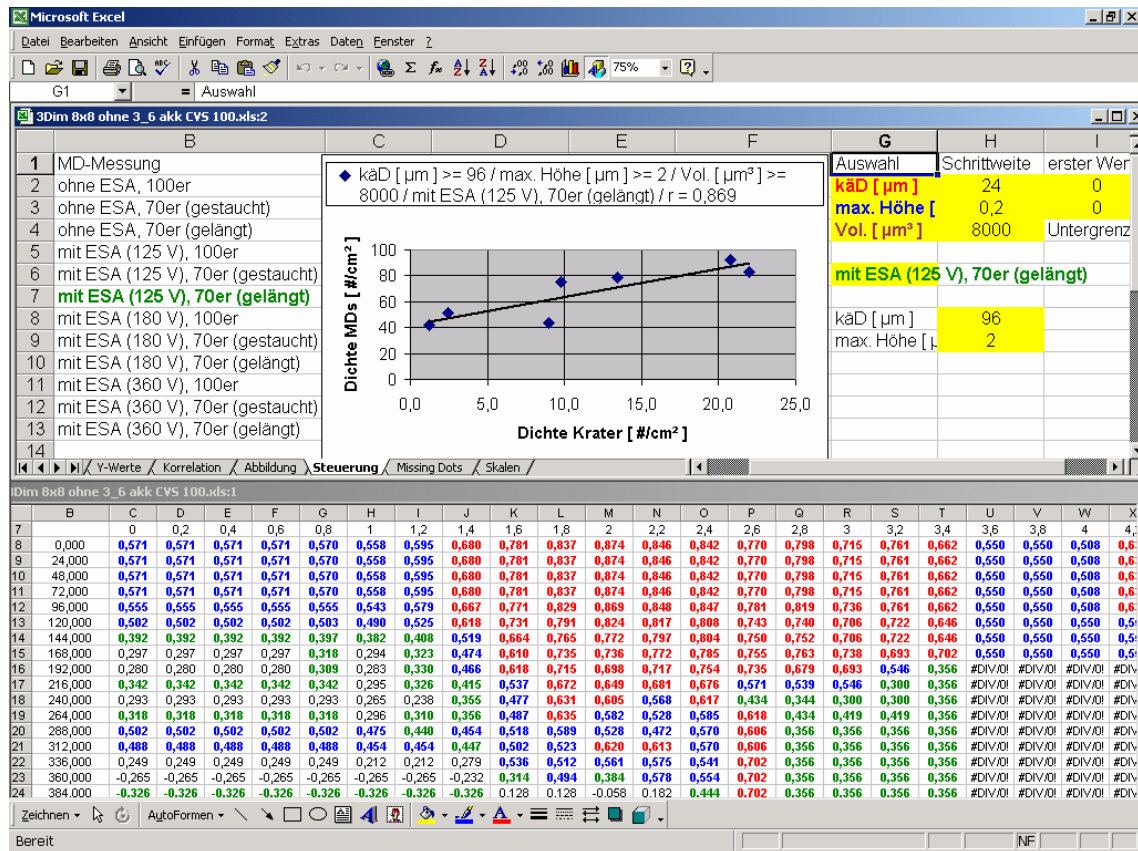


Figure 11: Excel program for multidimensional frequency distributions [8]

In the upper half of the figure all parameters, which result in the correlation coefficients in the lower half can be defined. In this example the histogram for the diameter and the depth is shown. When choosing a limit value for another parameter (e.g. volume) the histogram can get even a third dimension. All correlation coefficients which are higher than 0.6 are automatically coloured red to distinguish the strong interrelations. Furthermore it can be chosen at which ESA-settings and at which screens (upper left corner) the correlations shall be calculated. With an included diagram where the concentration of the craters is correlated with the concentration of the missing dots single interrelations can be diagrammed.

The following figures show two examples of correlations for different ESA-settings. The samples SC-3 and SC-6 are marked (cp. 4.3) and not included in the calculation of the correlation coefficient r. The interrelation of the values in Figure 12 and 13 are statistically assured with a probability of higher than 99 %. Furthermore the correlation with  $r = 0,882$  would persist with 8 values (with SC-3), too.

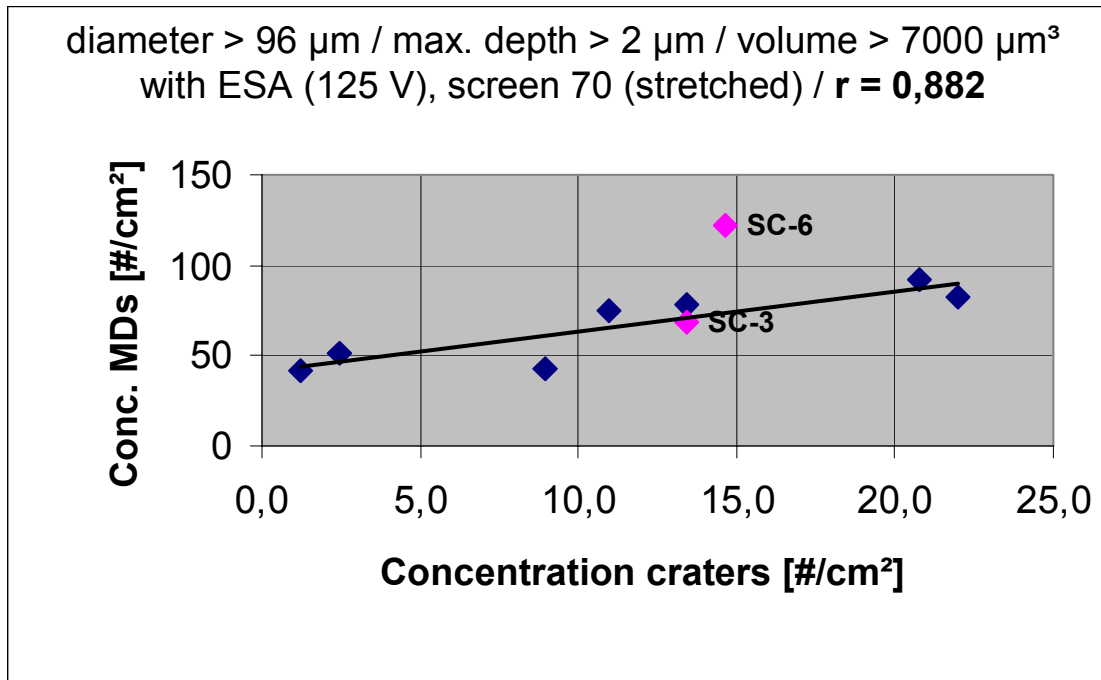


Figure 12: Combination of limit values: depth, diameter and volume at ESA 125 V [8]

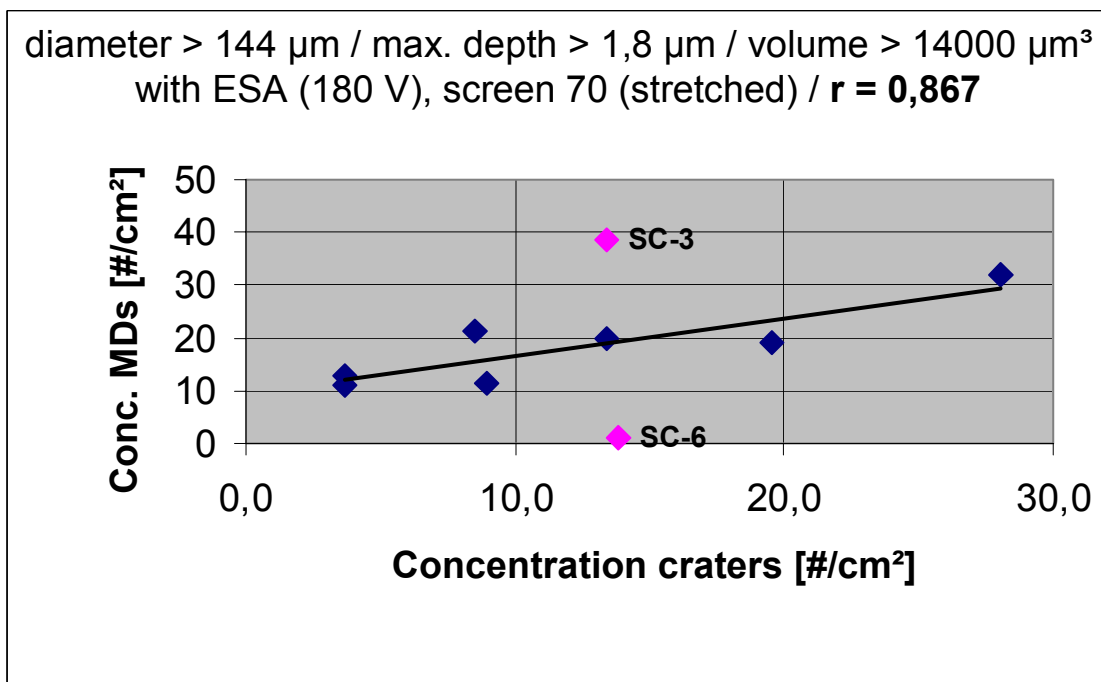


Figure 13: Combination of the three limit values at ESA 180 V [8]

It was generally established that there were only few interrelations at ESA 360 V. In contrast to the correlations of ESA-voltages from 0-180 V they were not frequent enough and no correlations out of a larger array of good correlations in the frequency functions.

## 6 Discussion of the results and conclusions

Through the advanced analysis of the crater statistics it was possible to find very good interrelationships between the surface topography of the papers and the number of missing dots. Especially for lower ESA-settings the correlations have been very strong. At ESA 360 V only few interrelations could be found, which was probably due to the increasing influence of the electric properties at high ESA-voltages.

The investigation of the MD-topographies has shown that parameters such as crater depth, crater volume, slope and concentration of craters correlate very well with the number of missing dots. Through the average surface finish sRa no differentiation of the investigated SC(A)-papers was possible, and the papers were partly ranked inversely to their printability by this value.

The strongest interrelations have been found by the combination of different parameters. Thus, in addition to the crater depth also the diameter and volume of craters are decisive for the generation of missing dots. When these three values are combined and correlated with the number of missing dots, stronger relationships than with only one limit value can be found. As a result the characteristics of craters which can cause missing dots with a high probability at the different ESA settings have been found. The deepening which cause missing dots have an average depth of 2-5  $\mu\text{m}$  and diameters between 50-250  $\mu\text{m}$ . When ESA is used bigger craters as regards depth and diameter are necessary to cause missing dots. Through the advanced analysis of the crater statistics Stora Enso Research Mönchengladbach has done a further step to forecast the printability of unprinted paper in the rotogravure process.

However, not all missing dots can be explained and described by means of surface topography. Non-topographic factors, such as electric properties of papers (especially when using the ESA), fibre and filler distribution, ink absorbency or microscopic compressibility can also have an influence on printability as regards missing dots. Paper independent factors (e.g. printing ink or printing machine) may also have a certain influence on missing dots. Therefore, investigations in these fields, together with the results of topography analysis, are necessary in order to draw clear and general conclusions regarding the causes of missing dots in rotogravure printing.

## 7 References

|     |   |
|-----|---|
| [1] | A CAMPO, F.W.: <i>Untersuchungen zum Zusammenhang zwischen Oberflächenstruktur und Missing Dots</i> . Stora Enso internes Memo 03-7035 RCM (3/2003)   |
| [2] | ANTOINE, C.; MANGIN, P.J.; VALADE, J.L.(1995): <i>The Influence of Underlying Paper Surface Structure on Missing Dots in Gravure</i> . In: <i>Advances in printing science and technology</i> (ed.:Bristow, J.A.) Chichester: 401-414 |
| [3] | ATOS GmbH: <i>Kurzanleitung zum Betrieb des PL<math>\mu</math> und Strukturvermessung an Papieroberflächen und Pl<math>\mu</math> User Manual</i> (2002).   |
| [4] | BÖTTGER, J.: <i>Influence of electrostatic charge (ESA) on number of missing</i>  |



|      |  |
|------|--|
|      | <i>dots.</i> Stora Enso Quality Meeting 02.04.2003   |
| [5]  | JERNSTRÖM, E.; AHONEN, A.: <i>Bedruckbarkeitsprüfung für den Tiefdruck.</i> Wochenblatt für Papierfabrikation 125 (1997), Nr. 1, S. 12-15  |
| [6]  | JOHANSSON, P.-A.; HANSSON, P.: <i>A new method for the simultaneous measurement of surface topography and ink distribution on prints.</i> STFI, Stockholm, Sweden. <a href="http://www.ind.tno.nl/en/cost_action_e11/index.html">http://www.ind.tno.nl/en/cost_action_e11/index.html</a> |
| [7]  | JÜHE, H.-H.: <i>Rotogravure Printing-Nip.</i> Stora Enso Quality Meeting 02.04.2003  |
| [8]  | MARTORANA, E.: <i>Untersuchungen zum Zusammenhang von Oberflächentopographie und Missing Dots bei SC-Papieren.</i> Diplomarbeit Fachhochschule München und Stora Enso Corporate Research Mönchengladbach (2/2005).   |
| [9]  | MOREAU-TABICHE, S. (2003): <i>Comparison of different developed methods for surface characterisation</i> [online]. Centre Technique du Papier, Grenoble <a href="http://www.ind.tno.nl/en/cost_action_e11/index.html">http://www.ind.tno.nl/en/cost_action_e11/index.html</a>            |
| [10] | NEß, C.; BILLEB, T.: <i>Untersuchungen zur Bedruckbarkeit von SC-Papieren im Tiefdruck.</i> ipw 3/2000, Nr. 3, S. T40-T48  |
| [11] | NEß, C.; GÖTTSCHING, L.: <i>Zweidimensionale Erfassung der Oberflächenstruktur von Papier im Hinblick auf seine Bedruckbarkeit.</i> Das Papier 51 (1997), Nr. 3, S. 107-117  |
| [12] | PRAAST, H.; GÖTTSCHING, L.: <i>Analyse und Ursachen von Missing Dots im Tiefdruck.</i> Das Papier 47 (1993), Nr. 1, S. 12-19   |
| [13] | VEENSTRA, P. (2003): <i>The need to develop surface-measuring equipment</i> [online]. Veenstra Technological Advises, Assendelft, Netherlands <a href="http://www.ind.tno.nl/en/cost_action_e11/index.html">http://www.ind.tno.nl/en/cost_action_e11/index.html</a>                      |
| [14] | VOGT, M.; PRAAST, H.; GÖTTSCHING, L.: <i>Charakterisierung der Rauheit von Papier mittels eines Lasersensors.</i> Das Papier 49 (1995), Nr. 11, S. 663-670   |